Multi-walled Carbon Nanotubes/Manganese Dioxide Nano- flowers-like/Polyaniline Nanowires Nanocomposite Modified Electrode: A New Platform for a Highly Sensitive Electrochemical Impedance DNA Sensor

Tuan Chu (chuvantuan@utehy.edu.vn)
Hung Yen University of Technology and Education, Khoai Chau District
Luyen Thi Tran
Hanoi University of Science and Technology
Hoang Vinh Tran
Hanoi University of Science and Technology
Trung Tran
Hoa Binh University
Nghia Trong Nguyen
Hung Yen University of Technology and Education, Khoai Chau District
Dan Bui
Hung Yen University of Technology and Education, Khoai Chau District
Phu Quang Tran
Hung Yen University of Technology and Education, Khoai Chau District

Research Article

Keywords: DNA sensor, nanocomposite, polyaniline nanowires, multi-walled carbon nanotubes, manganese dioxide

Posted Date: March 12th, 2021

DOI: https://doi.org/10.21203/rs.3.rs-280743/v1

Multi-walled Carbon Nanotubes/Manganese Dioxide Nano-flowers-like/Polyaniline Nanowires Nanocomposite Modified Electrode: A New Platform for a Highly Sensitive Electrochemical Impedance DNA Sensor

Luyen Thi Tran [2], Hoang Vinh Tran [2], Trung Tran [3], Nghia Trong Nguyen [1], Dan Van Bui [1], Phu Quang Tran [1], Tuan Van Chu [1,*]

[1] Hung Yen University of Technology and Education, Khoai Chau District, Hung Yen Province, Vietnam

[2] School of Chemical Engineering (SCE), Hanoi University of Science and Technology, 1st Dai Co Viet Road, Hai Ba Trung District, Hanoi, Vietnam

[3] Hoa Binh University, Nam Tu Liem District, Hanoi, Vietnam

* Corresponding author:
Telephone: 84 221 3713283/Fax: 84 221 3713015
Email address: chuvantuan@utehy.edu.vn (Tuan Van Chu)

Abstract

We describe in this report a development of label-free electrochemical DNA sensor based on a novel nanostructured electrode of multi-walled carbon nanotubes (MWCNTs)/ nano-flowers-like manganese dioxide (MnO_2)/polyaniline nanowires (PANi NWs) nanocomposite. The nanocomposite was synthesized in-situ onto an interdigitated platinum microelectrode (Pt) using a combination of chemical and electrochemical synthesis methods: chemical preparation of MWCNTs/MnO_2 and electropolymerization of PANi NWs. The fabricated MWCNTs/MnO_2/PANi NWs was then used to develop a label-free electrochemical DNA sensor for a specific gene of *Escherichia coli* (*E.coli*) O157:H7 detection. The MWCNTs/MnO_2/PANi NWs modified Pt electrode's surface can facilitate for probe DNA strands immobilization and, therefore the electrochemical signal of the DNA sensors has been improved. The electrochemical impedance spectroscopy (EIS) measurements were conducted to investigate the output signals generated by the specific binding of probe and target DNA sequences. Obtained results indicated that the developed electrochemical biosensor can detect the target DNA in the linear range of 5 pM to 500 nM with a low limit of detection (LOD) at 4.42×10^{-13} M. The research results demonstrated that the MWCNTs/MnO_2/PANi NWs nanocomposite-based electrochemical DNA sensor has a great potential application to the development of highly sensitive and selective electrochemical DNA sensors to detect pathogenic agents.

Keywords: DNA sensor, nanocomposite, polyaniline nanowires, multi-walled carbon nanotubes, manganese dioxide

1. Introduction

In recent decades, conducting polymers have been attracted the much attention of scientists worldwide for biosensing applications thanks to their unique properties [1-4]. Pure conducting polymers are formed in various structures such as nanowires, nanotubes and nano-thin films to obtain a large surface area and a high efficiency [5, 6]. The combination of conducting polymers with dopants can provide additional advantages, such as high conductivity, large surface areas, environment-friendly features, stability and applicability in biosensors [7-9].

Nanocomposite materials created from conducting polymers such as polyaniline (PANi), polypyrrole (PPy), poly(3,4-ethylenedioxythiophene) (PEDOT), and inorganic nanomaterials have excellent characteristics that are not obtained by individual components, including high conductivity, high stability, and high electroactive surface area, leading to new promising applications [10-13]. These nanocomposites show advantageous properties of inorganic nanomaterials distributed in continuous polymer networks [14, 15] and improvement of specifications of conducting polymers, including changes in electron structure of polymer chains, enhancement of charge transfer, and changes in conductivity of polymer chains [16, 17]. Actually, several inorganic nanomaterials have been used to dope into the polymer networks, such as PANi/Ni [18], PANi/Au [19], PANi/WO_3 [20], PANi/Mn_2O_3 [21], PANi/MnO_2 [22] and PANi/MWCNTs [8] nanocomposites. In general, these nanocomposites can be synthesized by different techniques including chemical, electrochemical, photochemical and mechano-chemical methods and these developed materials have been applied for many applications such as energy storage, electrochemical biosensors, electrochemical sensors, FET-based biosensors, and coating and metal protecting [1]. To apply of the inorganic nanomaterial/conducting polymer nanocomposites for development of electrochemical biosensors, these fabricated nanomaterials have to be coated onto the electrodes using a drop-casting and/or an electrochemical method in-situ on the working electrode [2, 23]. In which, the electrochemical techniques are often used due

to well controlling and high reproducibility. For examples, several PANi nanocomposites-based sensitive electrochemical DNA sensors have been developed such as PANi-graphene nanocomposite [24], silver nanoparticles decorated PANi nanowires [2], carbon dot/ZnO nanorod/PANi composite [25], PANi/gold nanoparticles [26], Sm_2O_3 NPs-rGO/PANi composite [27]. These developed PANi-based electrochemical DNA sensors have shown sensitivity at nM to fM level for DNA detection, however, the fabrication steps are still laborious. Therefore, in this study, the MWCNTs/MnO_2/PANi NWs nanocomposite was synthesized in-situ on Pt microelectrodes by a novel combined chemical-electrochemical technique, and was used for the first time to develop a label-free electrochemical DNA sensor for rapid detection of pathogenic bacteria.

2. Experimentals

2.1. Chemicals and instrumentations

2.1.1. Chemicals

MWCNTs (110–170 nm in diameter, 5–9 μm in length, > 90 wt.%), aniline ($C_6H_5NH_2$, 99.5 wt.%), sulfuric acid (H_2SO_4, 98 wt.%), nitric acid (HNO_3, 68 wt.%), phosphate buffer solution (PBS), potassium permanganate ($KMnO_4$, 99 wt.%), and manganese (II) chloride tetrahydrate ($MnCl_2.4H_2O$, 98 wt.%) were purchased from Sigma Aldrich. The supporting chemicals such as $K_2Cr_2O_7$ (99 wt.%) and N_2 (99.9 wt.%) were of analytical grade. The DNA probe, the complementary and non-complementary DNA target sequences are listed in **Table 1**.

Table 1. The DNA sequences used in this study.

Probe:	5'-AACGCCGATACCATTACTTA-3'
Complementary target:	3'-TTGCGGCTATGGTAATGAAT-5'
Non-complementary target:	5'-AACGCCGATACCATTACTTA-3'

2.1.2. Interdigitated Pt electrodes

The interdigitated Pt microelectrodes were fabricated using a standard photolithography technique with a finger width of 10 µm and a gap size of 20 µm. The fabrication process was conducted by sputtering 10 nm Ti and 200 nm Pt on a 100 nm thick silicon dioxide (SiO_2) layer thermally grown on top of a silicon wafer. The configuration and fabrication process of these electrodes were discussed in our previous work [28].

2.1.3. Instrumentations

Scanning electron microscopy (SEM) images and energy dispersive X-ray spectroscopy (EDX) spectra of the synthesized materials were investigated using a Nova NanoSEM 450 microscope. The structure of the fabricated samples was examined using Fourier transform infrared spectroscopy (FT-IR) spectra measured with a Shimadzu IRAffinity-1S FTIR spectrometer. Electrochemical measurements were performed using the PGSTAT302N AutoLab electrochemical workstation (Netherlands). A three-electrode configuration consists of the interdigitated Pt electrode as a working electrode (WE), a Pt plate as a counter electrode (CE), and a Ag/AgCl electrode (SCE) in 3M KCl solution (Metrohm) as a reference electrode (RE).

2.2. Fabrication of MWCNTs/MnO_2/PANi NWs nanocomposite-based Pt microelectrodes

The multi-walled carbon nanotubes were firstly oxidized by a mixture of H_2SO_4/HNO_3 by following typical protocol: a 21.8 mg of MWCNTs was refluxed with 2 mL of mixture of 1:1 v/v of 68 wt.% HNO_3 and concentrated H_2SO_4 (98 wt.%) solution for 5 hours at 95 °C. Then the above mixture was rinsed with distilled water until the pH was neutral, and the residue was dried at 80 ^oC for 12 hours to obtained the denatured MWCNTs. Secondly, MWCNTs/MnO_2 was synthesized by dispersion of 5.45 mg of the denatured MWCNTs as black powder into 10 mL of distilled water using the ultrasonic process for 10 minutes. The suspension was then implanted into a water bath

at 75 ^{o}C under continuous stirring with the fixed rate at 500 rpm using an IKA magnetic stirrer. After that, a 2 mL of $MnCl_2$ solution (containing 37.2 mg $MnCl_2.4H_2O$) was added into a reaction vessel and the mixture was stirred at 75 ^{o}C for 15 minutes. Then, 2 mL of $KMnO_4$ solution (containing 19.8 mg $KMnO_4$) was dropped slowly into the above mixture at a temperature of 75 °C, under the stirring condition for 2 hours. The MWCNTs/MnO_2 nanocomposite was collected by a centrifugation at 3000 rpm and then it was rinsed many times with distilled water until pH neutral. The MWCNTs/MnO_2 was re-dispersed into 10 mL distilled water to use.

Before fabrication of the nanocomposite onto the surface, Pt microelectrodes were treated in a solution of saturated $K_2Cr_2O_7$ in H_2SO_4 0.5 M and then electro-chemically activated in a solution of 0.5 M H_2SO_4 at the voltage range from –1.5 V to 2.2 V and the scanning rate of 50 mV s^{-1}. Then, 3 µL of the MWCNTs/MnO_2 sample was drop-casted onto the surface of the Pt microelectrode, and it was dried in the air under an infrared lamp. Finally, electrosynthesis of PANi NWs on the Pt/MWCNTs/MnO_2 electrodes was performed. The electrolyte solution containing 0.05 M aniline and 0.5 M H_2SO_4 was blown with N_2 gas for 15 minutes to purge the dissolved oxygen. The electropolymerization was conducted at room temperature using the chronoamperometry (CA) method with an applied voltage of 0.9 V vs. Ag/AgCl RE. After that, the MWCNTs/MnO_2/PANi NWs nanocomposite fabricated on the Pt WE was rinsed with deionized water, and was dried at room temperature.

2.3. Preparation of MWCNTs/MnO_2/PANi NWs-based electrochemical DNA sensors and DNA hybridization detection

To prepare of electrochemical DNA sensor, a 10 µL of 10 µM DNA probe in PBS solution was dropped onto the surface of the Pt/MWCNTs/MnO_2/PANi NWs electrodes. The probe DNA immobilization process was kept for 2 hours at room temperature. Then these electrodes were rinsed with deionized water to remove DNA sequences which did not bind or had weak linkages

with the MWCNTs/MnO_2/PANi NWs nanocomposite. The DNA sensors were then dried in the air and were ready for further experiments. To confirm the immobilization of DNA capture probe, the fluorescent technique was conducted to determine the efficiency of the DNA probe immobilization on the surface of the Pt/MWCNTs/MnO_2/PANi NWs electrode. 10 µL of 10 µM DNA probe with fluorescent components in PBS solution was dropped onto the surface of the Pt/MWCNTs/MnO_2/PANi NWs electrode, and was annealed for 2 hours at room temperature. After that, this electrode was rinsed by PBS buffer solution (pH 7.4) and deionized water, and was dried. Finally, it was observed with a 40x objective lens and a 10x ocular lens, at 343–390 nm wavelength, in randomly selected locations where DNA probe chains were immobilized.

For DNA target detection, the electrochemical impedance spectroscopy (EIS) spectra in the electrolyte solution consisting of 0.1 M KCl and 0.1 M PBS buffer (pH 7.4) at the frequency range from 10^4 Hz to 0.1 Hz, a DC potential of 230 mV and an AC potential of 5 mV (vs. Ag/AgCl (SCE) as RE) of the DNA sensors before and after hybridization with the DNA target with different concentrations (from 5 pM to 500 nM) were recorded. On EIS spectra, the increase of the electron transfer resistance ΔR_{ct} ($\Delta R_{ct} = R_{ct,i} - R_{ct,0}$) is used as the DNA hybridization signal, where $R_{ct,0}$ and $R_{ct,i}$ are the electron transfer resistances in the absence and presence of the DNA target, respectively.

3. Results and discussion

3.1. Characterization of MWCNTs/MnO_2/PANi NWs-modified Pt electrodes

Figure 1 shows the chronoamperometry (CA) results of an unmodified Pt microelectrode (curve a), a MWCNTs modified Pt microelectrode (Pt/MWCNTs) (curve b) and a MWCNTs/MnO_2 modified Pt microelectrode (Pt/MWCNTs/MnO_2) (curve c) in 0.5 M H_2SO_4 solution containing of 0.05 M aniline monomer during electropolymerization. It can be seen that the response currents were increased vs. electropolymerization time indicating that the PANi was successfully deposited

onto the Pt and modified Pt electrodes. Moreover, **Fig. 1** also shows the highest response current in the case of the Pt/MWCNTs/MnO_2 electrode and the lowest with the unmodified Pt electrode, which imply that the MWCNTs and MWCNTs/MnO_2 nanomaterials have improved the PANi growth on the electrodes via enhancing conductivity and electroactive surface [20, 24, 26].

Figure 2 shows the cyclic voltammogram (CV) results (**Fig. 2A**) and the electrochemical impedance spectroscopy (EIS) spectra (**Fig. 2B**) of the Pt microelectrode (curve a), PANi nanowires grown directly on the unmodified Pt microelectrode (Pt/PANi NWs, curve b), PANi nanowires grown on the MWCNTs modified Pt microelectrode (Pt/MWCNTs/PANi NWs, curve c) and PANi nanowires grown on the MWCNTs/MnO_2 modified Pt microelectrode (Pt/MWCNTs/MnO_2/PANi NWs, curve d). It can be seen in **Fig. 2A** that the PANi has improved the electroactivity of the Pt microelectrode by comparing curve b and curve a. In addition, the MWCNTs/MnO_2/PANi NWs nanocomposite has a stronger improvement in the electrochemical activity than that of the MWCNTs/PANi NWs or the PANi NWs as comparing curve d with curve c and with curve b. The EIS spectra in **Fig. 2B** agree with the CV data in **Fig. 2A**, i.e., the R_{ct} values were arranged as following: R_{ct} (Pt/MWCNTs/MnO_2/PANi NWs) < R_{ct} (Pt/MWCNTs/PANi NWs) < R_{ct} (Pt/PANi NWs). These results indicate clearly that the MWCNTs/MnO_2/PANi NWs has the highest electroactive and reduces the electron transfer resistance (R_{ct}), implying that the use of MWCNTs/MnO_2 to modify the Pt electrode has improved the electrical property of PANi NWs grown onto the electrode surface and has also enhanced the electrochemical active area for DNA capture probe immobilization, therefore the MWCNTs/MnO_2/PANi NWs nanocomposite can improve the electrochemical signal for electrochemical DNA sensors.

Figure 3 shows the SEM images of MWCNTs (**Fig. 3A**), PANi NWs (**Fig. 3B**), MWCNTs/PANi NWs (**Fig. 3C**), MWCNTs/MnO_2 (**Fig. 3D**) and MWCNTs/MnO_2/PANi NWs (**Fig. 3E** and **Fig. 3F**) modified on the surface of the Pt microelectrodes. It can be seen that the MWCNTs are highly

uniform with diameters ranging from 100 to 200 nm (**Fig. 3A**). **Fig. 3B** shows the PANi NWs with 150–160 nm in diameters which were formed directly on the Pt electrodes by the CA method. The size of the PANi NWs is uniform, and the nanowires are distributed throughout the surface of the WE. Moreover, it can be seen in **Fig. 3C** that, the obtained PANi NWs are relatively uniform and distributed on the MWCNTs layer. On the other hand, **Fig. 3D** shows that the MWCNTs are surrounded by the MnO_2 material with the unique flower-like structure. Finally, it can be seen in **Fig. 3E** and **Fig. 3F**, the MWCNTs/MnO_2/PANi NWs nanocomposite was successfully synthesized in-situ on the Pt microelectrodes. The PANi NWs layer which was formed by the electrochemical method, covers the surface of the MWCNTs/MnO_2 film. In the fabrication of the electrochemical DNA sensors, the DNA probe immobilization on the electrode surface and the ability of the sensors to detect DNA target depend on compositions and surface structures of the materials modified the WE. In this study, the PANi NWs contain MWCNTs/MnO_2 as an impurity component. The MWCNTs tubes are surrounded with the flower-like MnO_2 blocks, and are distributed in the PANi nanowires. Polymers are not soluble, however, SO_4^{2-} ions in H_2SO_4 solution create bonds with PANi NWs and then increase polarity, so the distribution process of MWCNTs/MnO_2 into PANi nanowires is facilitated. The nanocomposite obtained through MWCNTs/MnO_2 bound to the wall of PANi nanowires, has a soft, porous, regular and specific structure. This structure has attracted the attention of researchers, and is found highly suitable for application in the development of DNA sensors.

The EDX spectra in **Fig. 4A** shows relatively the composition of the elements in samples of PANi NWs, MWCNTs/PANi NWs, MWCNTs/MnO_2/PANi NWs, MWCNTs/MnO_2 and MWCNTs on the Pt microelectrode surfaces (**Fig. 4A**, from curve a to curve e, respectively). As can be seen in **Fig. 4A**, carbon element (C), which is a constituent of MWCNTs and PANi NWs as well, was observed in all samples at position of 0.27 keV. In **Fig. 4A** (from curve a to curve c), the nitrogen

(N), oxygen (O), and sulfur (S) elements which are constituents of PANi NWs, were observed at energy levels of 0.39, 0.53 and 2.31 keV, respectively. These results can be explained that H_2SO_4 was doped into PANi NWs, leading to the appearances of S and O elements in the EDX spectra. When H_2SO_4 was doped into PANi NWs, cations which are formed at the imine N atoms play the role for the electronic conduction of PANi [29, 30]. Thus, in the electrochemical DNA sensor development, doping PANi with H_2SO_4 can improve the conductivity of PANi NWs, so the efficiency of information transmission from DNA hybridization to the transducer will be enhanced. On the other hand, in **Fig. 4A** from curve c to curve d, the manganese (Mn) element which is a constituent of MnO_2 was observed at 0.63 keV. These results indicate that the MWCNTs/MnO_2 and MWCNTs/MnO_2/PANi NWs nanocomposites were successfully synthesized on the Pt electrode surface. **Figure 4B** displays the FT-IR spectra of PANi NWs, MWCNTs/PANi NWs, MWCNTs/MnO_2/PANi NWs, MWCNTs/MnO_2, and MWCNTs (from curve a to curve e, respectively) obtained on the surface of the Pt microelectrodes. It can be seen in **Fig. 4B**, in the cases of MWCNTs/MnO_2/PANi NWs (curve c), MWCNTs/MnO_2 (curve d) and MWCNTs (curve e), the bands which characterize of the MWCNTs are observed. The band at 1015 cm^{-1} is assigned to the C–O stretching mode of the carboxylic acid group formed on the side wall of the MWCNTs [31]. Thus, the MWCNTs were oxidized. Besides, the band at 1144 cm^{-1} is attributed to the C–C stretching mode [32]. On the other hand, for the cases of PANi NWs (curve a), MWCNTs/PANi NWs (curve b), and MWCNTs/MnO_2/PANi NWs (curve c), the bands which characterize the PANi material appear. The bands attributed to the benzenoid (N–B–N) and quinoid (N=Q=N) ring stretching modes are observed at 1485 and 1574 cm^{-1}, respectively [33, 34]. Moreover, in the case of the obtained MWCNTs/MnO_2/PANi NWs nanocomposite (**Fig. 4B,** curve c), the peak intensity ratio of benzenoid/quinoid increases in comparison with the cases of the PANi NWs and MWCNTs/PANi NWs materials (**Fig. 4B**, curve a and curve b, respectively). This result can be explained that the addition of dopant components (MWCNTs/MnO_2) causes the transfer of part of

quinoid rings to benzenoid rings, leading to an interesting result that the conductivity of the obtained nanocomposite will increase. Besides, the bands associated with the C–N stretching and bending modes are observed at 1300 and 1243 cm^{-1} [33, 34]. The band observed at 3216 cm^{-1} is assigned to the N–H stretching mode [33]. And, the band associated with the S–O vibration mode is also found at 701 cm^{-1} [35]. These results indicate that in these samples (**Fig. 4B**, from curve a to curve c), the PANi material was formed, and H_2SO_4 was doped into PANi NWs. So, the above FT-IR spectra demonstrate that the MWCNTs/MnO_2/PANi NWs nanocomposite was successfully fabricated on the Pt microelectrode. These results are totally suitable with the electrochemical signals (CA data, CV spectra and EIS results) and EDX results as well. Moreover, in the synthesized MWCNTs/MnO_2/PANi NWs nanocomposite (**Fig. 4B**, curve c), the MWCNTs component was oxidized, and the PANi NWs component existed mainly in the emeraldine form which is the most conductive form of the PANi material.

3.2. Direct immobilization of DNA probe on Pt/MWCNTs/MnO_2/PANi NWs electrodes

The electrochemical impedance spectroscopy (EIS) measurements were used to investigate the efficiency of the DNA probe immobilization on the Pt/MWCNTs/MnO_2/PANi NWs electrode due to the electrical impedance changes of the electrode surface caused by the immobilization process of DNA capture probe strands. **Figure 5A** shows the Nyquist plots of the Pt/MWCNTs/MnO_2/PANi NWs electrodes before (curve a) and after (curve b) DNA capture probe immobilization. In comparison with the case that there is only the MWCNTs/MnO_2/PANi NWs nanocomposite deposited on the working electrode surface (**Fig. 5A, curve a**), the impedance of the sensor after DNA probe immobilization increases significantly (**Fig. 5A, curve b**). It can be seen in **Fig. 5A**, the charge transfer resistance (R_{ct}) of the Pt/MWCNTs/MnO_2/PANi NWs electrode before DNA probe immobilization is of 0.26 kΩ, which increases to 34.15 kΩ after DNA probe immobilization. This result demonstrates that the immobilization of DNA probe strands onto

the Pt/MWCNTs/MnO_2/PANi NWs electrode surface was conducted effectively. The obtained MWCNTs/MnO_2/PANi NWs structure with soft and porous surface characteristics is favorable for the immobilization process of DNA probe onto the electrode due to amino groups of PANi NWs and carboxylic groups of denatured MWCNTs can create bonds with phosphate groups of DNA strands [36]. To verify the immobilization of DNA capture probe strands onto the Pt/MWCNTs/MnO_2/PANi NWs electrodes, the fluorescent microscopy images have also been taken. The inserted figures (i) and (ii) in **Fig.5A** show the surface of the two Pt/MWCNTs/MnO_2/PANi NWs electrodes in absence and presence of DNA probe strands, respectively. It can be seen in the inserted figure (i), there is only the MWCNTs/MnO_2/PANi NWs nanocomposite which has no light spots. Inversely, in the inserted figure (ii), there are plenty of light spots as blue colour which are attributed to immobilized DNA strands. This result indicates that the DNA probe immobilization was performed effectively onto the modified electrode surface. After many cleaning steps using PBS buffer solution (pH 7.4) and deionized water, DNA probe sequences maintain bonds with the surface of the MWCNTs/MnO_2/PANi NWs nanocomposite. In comparison with other DNA immobilization methods, in this study, the DNA immobilization technique which was conducted in-situ on the electrode surface modified by the MWCNTs/MnO_2/PANi NWs nanocomposite is simple, convenient and effective [26, 37]. In addition, the MWCNTs/MnO_2/PANi NWs nanocomposite with high conductivity also plays an important role in enhancing of signal transmission from DNA hybridization to the transducer, thus, the sensibility of the electrochemical DNA sensor is expected to be improved significantly.

3.3. Detection of E.coli DNA target using MWCNTs/MnO_2/PANi NWs-based electrochemical DNA sensors

The selectivity of the DNA sensor based on the Pt/MWCNTs/MnO_2/PANi NWs electrode has been evaluated. **Fig. 5B** shows the Nyquist plots of the DNA sensor before (curve a) and after (curve

b) hybridization with a 50 nM of non-complementary DNA target solution. It can be observed that there was only a slight change in the R_{ct} with an increase about 2.50 kΩ in R_{ct}. This change was too small when compared with the case of complementary DNA target, the ΔR_{ct} value was 31.00 kΩ at 50 nM complementary DNA target (**Fig. 5C**, curve f). These data imply the selective property of this proposed DNA sensor.

The electrochemical impedance spectroscopy (EIS) is an useful technique for DNA sensing due to the electrical impedance changes of the electrode surface during the hybridization of DNA capture probe strands vs. complementary DNA target strands. **Fig. 5C** shows Nyquist impedance spectra of the Pt/MWCNTs/MnO_2/PANi NWs/DNA probe electrodes conducted in the electrolyte solutions with different concentrations of complementary DNA target (from 5 pM to 500 nM). As can be observed, specific hybridization between DNA target (in the electrolyte solution) and DNA probe (on the sensor surface) led to changes of the measured impedance signals. The impedance values of the DNA sensors in the presence of DNA target (from curve b to curve g) increase significantly in comparison with the impedance of the DNA sensor in the absence of DNA target (curve a). These results can be explained that DNA sequences contain negatively charged phosphate groups while the fabricated MWCNTs/MnO_2/PANi NWs nanocomposite is a conducting material with p-type charge carriers (holes). Thus, with the presence of DNA target in the electrolyte solution, the DNA hybridization occurring on the sensor surface, leads to reduction of the density of the charge carriers of the MWCNTs/MnO_2/PANi NWs nanocomposite, so, the conductivity is decreased and the impedance of the sensor is increased. The impedance spectra can be simulated by equivalent electric circuits. In this study, the EIS results fit well with the Randles equivalent circuit (**Fig. 5D**, inserted figure), which includes solution resistance (R_s), charge transfer resistance (R_{ct}), constant phase element (CPE) and Warburg diffusion coefficient (W). The R_s value depends on the electrolyte solution. The W value depends on the diffusion process that is exhibited by a linear region at low frequency range on the EIS spectrum. The presence of the CPE

value can be explained by the fact that, an electrochemical system has not an ideal capacitor due to the roughness of the sensor surface which is related to the porous characteristic of the MWCNTs/MnO_2/PANi NWs structure. Finally, the R_{ct} value that is exhibited by a semicircle region at high frequency range on the EIS spectrum, characterizes the charge transfer process. This value depends on changes of the sensor surface where DNA hybridization happens, so it is selected as the output signal for DNA target detection. The ΔR_{ct} values of the DNA sensors corresponding to different concentrations of complementary DNA target which have been used for the hybridization, are presented in the calibration curve (**Fig. 5D**). As it shown in the **Fig. 5D,** a good linear relationship between the ΔR_{ct} and the logarithm of the DNA target concentration in the range from 5.0×10^{-12} M to 5.0×10^{-9} M is obtained. The linear equation is ΔR_{ct} (kΩ) = $6.1259 \times \log C_{DNA\ target}$ (nM) + 76.8340 with the correlation coefficient of $R^2 = 0.9704$. The detection limit (LOD) was estimated of 4.42×10^{-13} M (at S/N >3) [38].

Table 2. Comparison of the fabricated electrochemical DNA sensor with some ones in the previous studies.

Surface modification	Synthesis method	Linear range (M)	Detection limit (M)	Reference
MWCNTs	Chemical method Drop-casting	1.0×10^{-9}–1.0×10^{-8}	1.0×10^{-9}	[28]
GS*/PANi film/AuNPs	Chemical method Drop-casting	1.25×10^{-12}–5×10^{-8}	2.5×10^{-13}	[39]
GS*/PANi film/AuNPs	Drop-casting Electrochemical method	1.0×10^{-11}–1.0×10^{-9}	2.11×10^{-12}	[37]
PPy–PANi–Au film	Combined chemical-electrochemical method	1.0×10^{-13}–1.0×10^{-6}	1.0×10^{-13}	[15]
MnO_2/chitosan film	Chemical method Drop-casting	2.0×10^{-11}–2.0×10^{-6}	1.0×10^{-12}	[40]
MWCNTs/MnO_2/PANi NWs	Combined chemical-electrochemical method	5.0×10^{-12}–5.0×10^{-9}	4.42×10^{-13}	This work

*GS: Graphene sheets

The electrochemical DNA sensor based on the MWCNTs/MnO_2/PANi NWs nanocomposite in this work can be competitive with some ones in the previous reports in the literature in terms the

linear range of detection and LOD as well (**Table 2**). Moreover, it is noteworthy that the DNA sensor based on the Pt/MWCNTs/MnO_2/PANi NWs microelectrodes required a very small volume of the DNA sample (only 10 μL) for the DNA capture probe immobilization. In addition, the DNA capture probe immobilization and DNA target hybridization processes can be carried-out at room temperature with the simple protocols. These properties indicated that the Pt/MWCNTs/MnO_2/PANi NWs microelectrodes can be used as an effective platform for development of the selective and sensitive DNA sensors for further applications.

4. Conclusions

The MWCNTs/MnO_2/PANi NWs nanocomposite was successfully fabricated in-situ onto the Pt electrodes using a combination of chemical-electrochemical techniques: chemical synthesis of MWCNTs/MnO_2 and electrosynthesis of PANi NWs. The SEM images have demonstrated that the MWCNTs/MnO_2/PANi NWs membrane modified onto Pt microelectrode has an uniform, soft and porous structure with a large specific surface area. The DNA probe strands can be effectively immobilized onto Pt/MWCNTs/MnO_2/PANi NWs electrodes' surface which can be directed to DNA target detection. Under optimal experimental conditions, the established EIS-based DNA sensor can be used to quantify specific DNA of E.coli O157:H7 based on the linear relationship between ΔR_{ct} and the logarithm of the DNA target concentration in the range from 5.0 pM to 5.0 nM with a detection limit of 0.442 pM. The obtained MWCNTs/MnO_2/PANi NWs nanocomposite can be a potential material for biosensing applications to detect pathogenic agents.

Author contribution statement

Luyen Thi Tran: Investigation.

Hoang Vinh Tran: Writing - review & editing.

Phu Quang Tran: Investigation.

Dan Van Bui: Investigation,

Nghia Trong Nguyen: Formal analysis.

Trung Tran: Formal analysis.

Tuan Van Chu: Supervision, Writing - review & editing.

Conflict of interest

There are no conflicts of interest to declare.

Acknowledgements

This research is funded by Vietnam National Foundation for Science and Technology Development (NAFOSTED) under grant number 103.02-2017.305.

References

[1] P. Singh and S. K. Shukla, Advances in polyaniline-based nanocomposites, *Journal of Materials Science,* **55**, 1331-1365 (2019).

[2] L. T. Tran, H. V. Tran, H. T. M. Dang, C. D. Huynh, and T. A. Mai, Silver Nanoparticles Decorated Polyaniline Nanowires-Based Electrochemical DNA Sensor: Two-step Electrochemical Synthesis, *Journal of The Electrochemical Society,* **167**, Article number 087508 (2020).

[3] E. A. de Oliveira Farias, S. S. Nogueira, A. M. de Oliveira Farias, M. S. de Oliveira, M. de Fátima Cardoso Soares, H. N. da Cunha, J. R. dos Santos Junior, D. A. da Silva, P. Eaton, and C. Eiras, A thin PANI and carrageenan−gold nanoparticle film on a flexible gold electrode as a conductive and low-cost platform for sensing in a physiological environment, *Journal of Materials Science,* **52**, 13365-13377 (2017).

[4] J. Chen, X. Zheng, Y. Li, H. Zheng, Y. Liu, and S.-i. Suye, A Glucose Biosensor Based on Direct Electron Transfer of Glucose Oxidase on PEDOT Modified Microelectrode, *Journal of The Electrochemical Society*, **167** (6), Article number 067502 (2020).

[5] T. X. Chu, V. P. Vu, H. T. Tran, T. L. Tran, Q. T. Tran, and T. L. Manh, Molecularly Imprinted Polyaniline Nanowire-Based Electrochemical Biosensor for Chloramphenicol Detection: A Kinetic Study of Aniline Electropolymerization, *Journal of The Electrochemical Society,* **167**, Article number 027527 (2020).

[6] T. L. Tran, T. X. Chu, D. C. Huynh, D. T. Pham, T. H. T. Luu, and A. T. Mai, Effective immobilization of DNA for development of polypyrrole nanowires based biosensor, *Applied Surface Science,* **314**, 260-265 (2014).

[7] C. S. Kushwaha and S. K. Shukla, Non-enzymatic potentiometric malathion sensing over chitosan-grafted polyaniline hybrid electrode, *Journal of Materials Science,* **54**, 10846-10855 (2019).

[8] H. T. Hien, H. T. Giang, T. Trung, and C. V. Tuan, Enhancement of biosensing performance using a polyaniline/multiwalled carbon nanotubes nanocomposite, *Journal of Materials Science,* **52**, 1694-1703 (2016).

[9] M. J. Dunlop and R. Bissessur, Nanocomposites based on graphene analogous materials and conducting polymers: a review, *Journal of Materials Science,* **55**, 6721-6753 (2020).

[10] Z. Rahimzadeh, S. M. Naghib, Y. Zare, and K. Y. Rhee, An overview on the synthesis and recent applications of conducting poly(3,4-ethylenedioxythiophene) (PEDOT) in industry and biomedicine, *Journal of Materials Science,* **55**, 7575-7611 (2020).

[11] R. Jain, N. Jadon, and A. Pawaiya, Polypyrrole based next generation electrochemical sensors and biosensors: A review, *TrAC Trends in Analytical Chemistry,* **97**, 363-373 (2017).

[12] B. Hatamluyi, Z. Es'haghi, F. Modarres Zahed, and M. Darroudi, A novel electrochemical sensor based on GQDs-PANI/ZnO-NCs modified glassy carbon electrode for simultaneous determination of Irinotecan and 5-Fluorouracil in biological samples, *Sensors and Actuators B: Chemical,* **286**, 540-549 (2019).

[13] G. Kaladevi, P. Wilson, and K. Pandian, Simultaneous and Selective Electrochemical Detection of Sulfite and Nitrite in Water Sources Using Homogeneously Dispersed Ag Nanoparticles over PANI/rGO Nanocomposite, *Journal of The Electrochemical Society*, **167** (2), Article number 027514 (2020).

[14] S. Weng, J. Zhou, and Z. Lin, Preparation of one-dimensional (1D) polyaniline–polypyrrole coaxial nanofibers and their application in gas sensor, *Synthetic Metals*, **160**, 1136-1142 (2010).

[15] J. Wilson, S. Radhakrishnan, C. Sumathi, and V. Dharuman, Polypyrrole–polyaniline–Au (PPy–PANi–Au) nano composite films for label-free electrochemical DNA sensing, *Sensors and Actuators B: Chemical,* **171-172**, 216-222 (2012).

[16] H. T. Hien, H. T. Giang, N. V. Hieu, T. Trung, and C. V. Tuan, Elaboration of Pd-nanoparticle decorated polyaniline films for room temperature NH_3 gas sensors, *Sensors and Actuators B: Chemical,* **249**, 348-356 (2017).

[17] P. Cavallo, D. F. Acevedo, M. C. Fuertes, G. J. A. A. Soler-Illia, and C. A. Barbero, Understanding the sensing mechanism of polyaniline resistive sensors. Effect of humidity on sensing of organic volatiles, *Sensors and Actuators B: Chemical,* **210**, 574-580 (2015).

[18] A. I. Inamdar, H. S. Chavan, H. Kim, and H. Im, Mesoporous Ni-PANI composite electrode for electrochromic energy storage applications, *Solar Energy Materials and Solar Cells,* **201**, Article number 110121 (2019).

[19] E. Saeb and K. Asadpour-Zeynali, Facile synthesis of TiO_2@PANI@Au nanocomposite as an electrochemical sensor for determination of hydrazine, *Microchemical Journal,* **160** (Part A), Article number 105603 (2021).

[20] S. Li, A. Liu, Z. Yang, L. Zhao, J. Wang, F. Liu, R. You, J. He, C. Wang, X. Yan, P. Sun, X. Liang, G. Lu, Design and preparation of the WO_3 hollow spheres@ PANI conducting films for room temperature flexible NH_3 sensing device, *Sensors and Actuators B: Chemical,* **289**, 252-259 (2019).

[21] A. H. Gemeay, R. G. Elsharkawy, and E. F. Aboelfetoh, Graphene Oxide/Polyaniline/Manganese Oxide Ternary Nanocomposites, Facile Synthesis, Characterization, and Application for Indigo Carmine Removal, *Journal of Polymers and the Environment,* **26**, 655-669 (2017).

[22] I. Izwan Misnon and R. Jose, Charge storage in the PANI–α-MnO_2 polymer–nanocomposite system, *Materials Today: Proceedings, **In Press*** (2020).

[23] R. Zhang, J. Qian, S. Ye, Y. Zhou, and Z. Zhu, Synthesis and Enhanced Electrochemical Activity of Ag-Pt Bimetallic Nanoparticles Decorated MWCNTs/PANI Nanocomposites, *Journal of Wuhan University of Technology-Mater. Sci. Ed.,* **33**, 1281-1287 (2018).

[24] Q. Gong, H. Han, H. Yang, M. Zhang, X. Sun, Y. Liang, Z. Liu, W. Zhang, J. Qiao, Sensitive electrochemical DNA sensor for the detection of HIV based on a polyaniline/graphene nanocomposite, *Journal of Materiomics,* **5**, 313-319 (2019).

[25] A. Pangajam, K. Theyagarajan, and K. Dinakaran, Highly sensitive electrochemical detection of *E. coli O157:H7* using conductive carbon dot/ZnO nanorod/PANI composite electrode, *Sensing and Bio-Sensing Research,* **29**, Article number 100317 (2020).

[26] R.-S. Saberi, S. Shahrokhian, and G. Marrazza, Amplified Electrochemical DNA Sensor Based on Polyaniline Film and Gold Nanoparticles, *Electroanalysis,* **25**, 1373-1380 (2013).

[27] N. Mohammadian and F. Faridbod, ALS genosensing using DNA-hybridization electrochemical biosensor based on label-free immobilization of ssDNA on Sm_2O_3 NPs-rGO/PANI composite, *Sensors and Actuators B: Chemical,* **275**, 432-438 (2018).

[28] N. T. Thuy, P. D. Tam, M. A. Tuan, A. T. Le, L. T. Tam, V. V. Thu, N. V. Hieu, N. D. Chien, Detection of pathogenic microorganisms using biosensor based on multi-walled carbon nanotubes dispersed in DNA solution, *Current Applied Physics,* **12**, 1553-1560 (2012).

[29] E. Song and J. W. Choi, Conducting Polyaniline Nanowire and Its Applications in Chemiresistive Sensing, *Nanomaterials (Basel),* **3**, 498-523 (2013).

[30] S. Wang, S. Lu, X. Li, X. Zhang, S. He, and T. He, Study of H_2SO_4 concentration on properties of H_2SO_4 doped polyaniline counter electrodes for dye-sensitized solar cells, *Journal of Power Sources,* **242**, 438-446 (2013).

[31] N. H. Metwally, G. R. Saad, and E. A. Abd El-Wahab, Grafting of multiwalled carbon nanotubes with pyrazole derivatives: characterization, antimicrobial activity and molecular docking study, *International Journal of Nanomedicine,* **14**, 6645-6659 (2019).

[32] N. S. Alghunaim, Optimization and spectroscopic studies on carbon nanotubes/PVA nanocomposites, *Results in Physics,* **6**, 456-460 (2016).

[33] G.-R. Li, Z.-P. Feng, J.-H. Zhong, Z.-L. Wang, and Y.-X. Tong, Electrochemical Synthesis of Polyaniline Nanobelts with Predominant Electrochemical Performances, *Macromolecules,* **43**, 2178-2183 (2010).

[34] M. H. Abdel Rehim, A. M. Youssef, H. Al-Said, G. Turky, and M. Aboaly, Polyaniline and modified titanate nanowires layer-by-layer plastic electrode for flexible electronic device applications, *RSC Advances,* **6**, 94556-94563 (2016).

[35] M. Trchová, I. Šeděnková, E. Tobolková, and J. Stejskal, FTIR spectroscopic and conductivity study of the thermal degradation of polyaniline films, *Polymer Degradation and Stability,* **86**, 179-185 (2004).

[36] N. Zhu, Z. Chang, P. He, and Y. Fang, Electrochemically fabricated polyaniline nanowire-modified electrode for voltammetric detection of DNA hybridization, *Electrochimica Acta,* **51**, 3758-3762 (2006).

[37] L. Wang, E. Hua, M. Liang, C. Ma, Z. Liu, S. Sheng, M. Liu, G. Xie, W. Feng, Graphene sheets, polyaniline and AuNPs based DNA sensor for electrochemical determination of BCR/ABL fusion gene with functional hairpin probe, *Biosensors and Bioelectronics,* **51**, 201-207 (2014).

[38] H. V. Tran, B. Piro, S. Reisberg, L. D. Tran, H. T. Duc, and M. C. Pham, Label-free and reagentless electrochemical detection of microRNAs using a conducting polymer nanostructured by carbon nanotubes: application to prostate cancer biomarker miR-141, *Biosensors and Bioelectronics,* **49**, 164-169 (2013).

[39] X. Chen, D. Zhou, H. Shen, W. Feng, H. Chen, and G. Xie, A Facile Electrochemical Biosensor for the Detection of microRNA Based on Graphene Sheets/Polyaniline/AuNPs, *International Journal of Material and Mechanical Engineering,* **4**, 24-28 (2015).

[40] Z.-M. Liu, Z.-J. Li, G.-L. Shen, and R.-Q. Yu, Label-Free Detection of DNA Hybridization Based on MnO_2 Nanoparticles, *Analytical Letters,* **42**, 3046-3057 (2009).

List of Figures

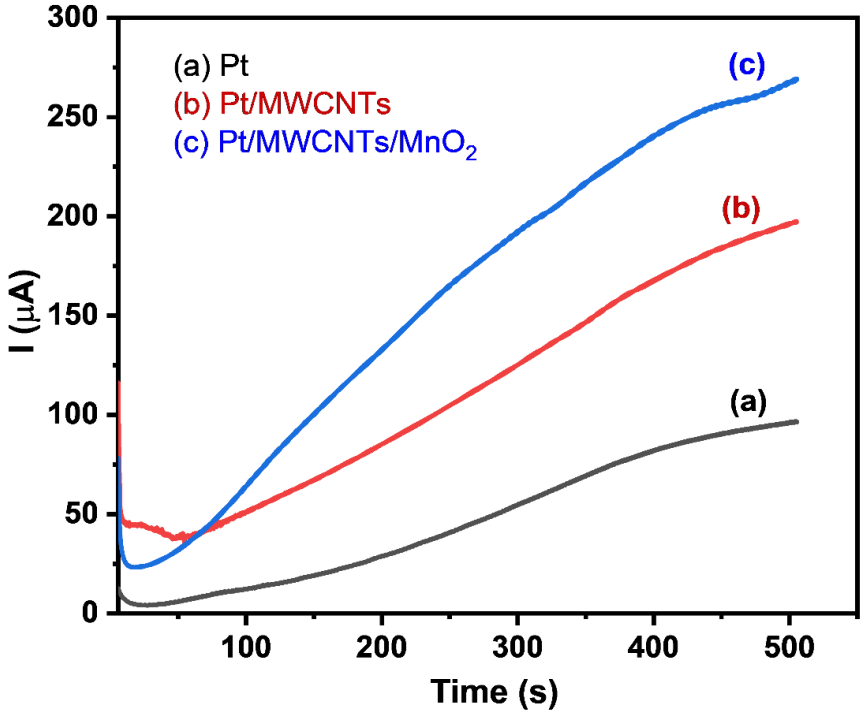

Figure 1. CA results of (a) a bare Pt electrode, (b) a MWCNTs modified Pt electrode (Pt/MWCNTs) and (c) a MWCNTs/MnO_2 modified Pt electrode (Pt/ MWCNTs/MnO_2). Experimental conditions: the CA curves were recorded in solution containing of 0.05 M aniline monomer and 0.5 M H_2SO_4 with an applied voltage of 0.9 V vs. SCE at room temperature.

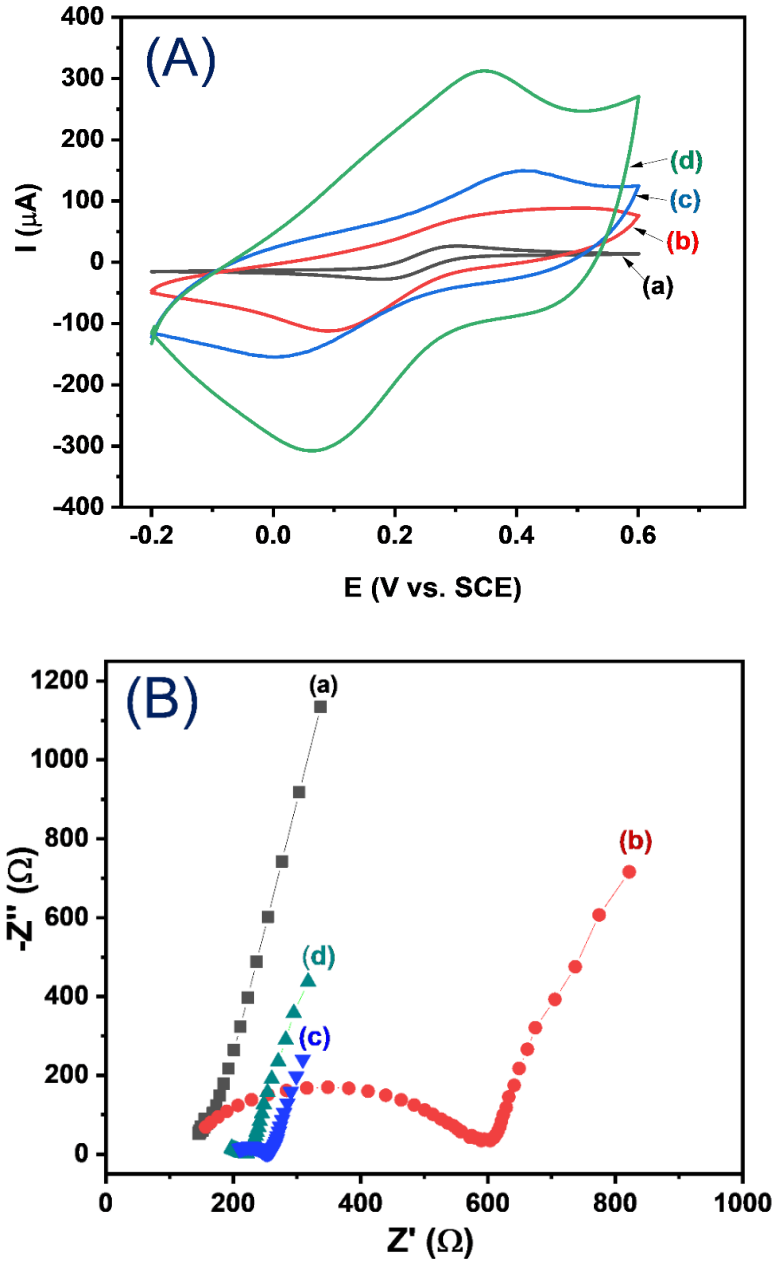

Figure 2. (A) CV results and (B) EIS spectra of (a) bare Pt electrode, and modified Pt electrodes with: (b) MWCNTs, (c) MWCNTs/PANi NWs and (d) MWCNTs/MnO_2/PANi NWs films. Experimental conditions: CV and EIS were measured in $K_3Fe(CN)_6/K_4Fe(CN)_6$ (0.005 M) and 0.1 M KCl solution. The CV was recorded at 25 mV s^{-1} scan rate. The EIS was measured with frequency range: 10^4 Hz to 0.1 Hz, E_{AC} = 5 mV and E_{DC} = 230 mV.

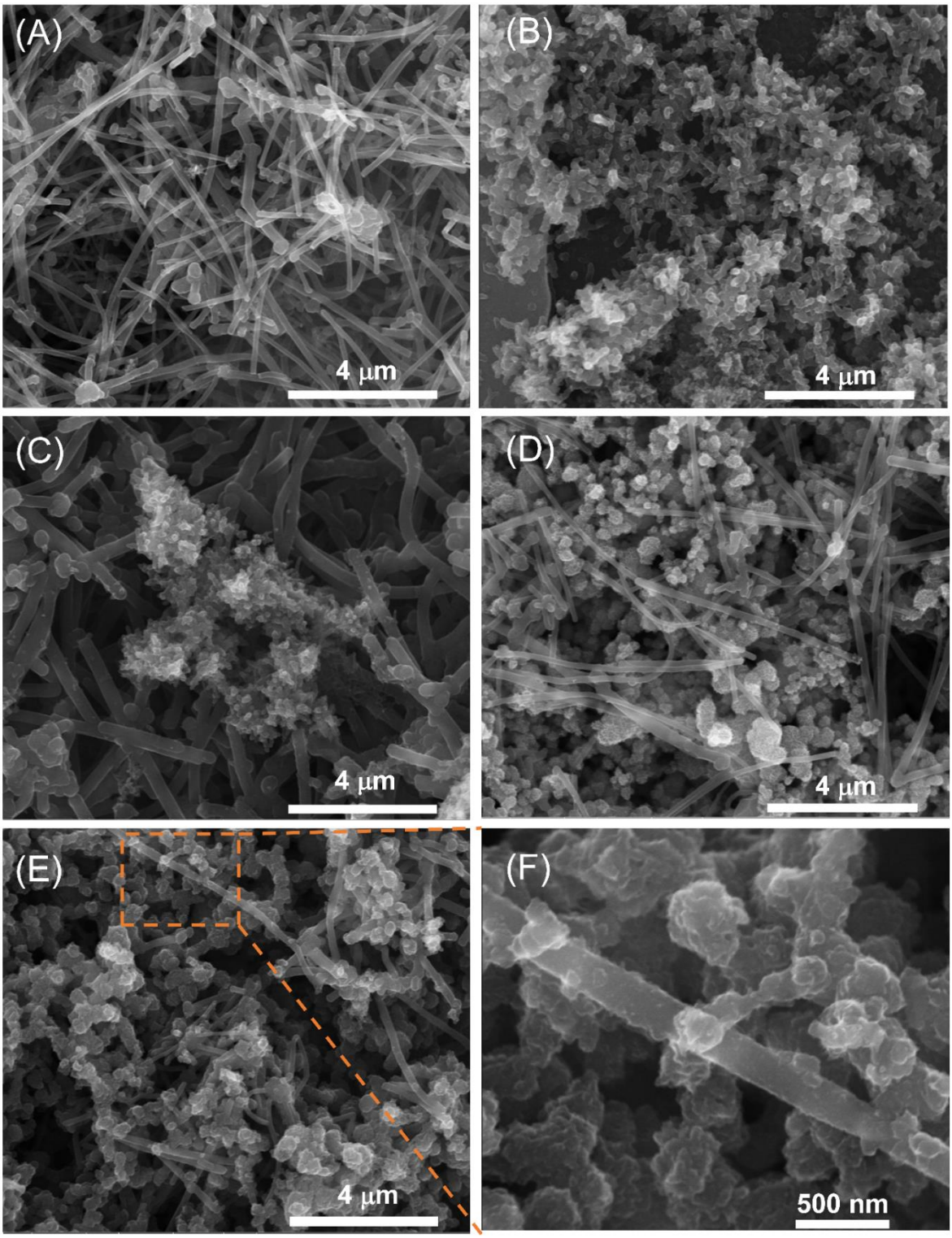

Figure 3. SEM images of (A) MWCNTs; (B) PANi NWs; (C) MWCNTs/PANi NWs; (D) MWCNTs/MnO_2; (E, F) MWCNTs/MnO_2/PANi NWs on the surface of the Pt electrodes with different magnifications.

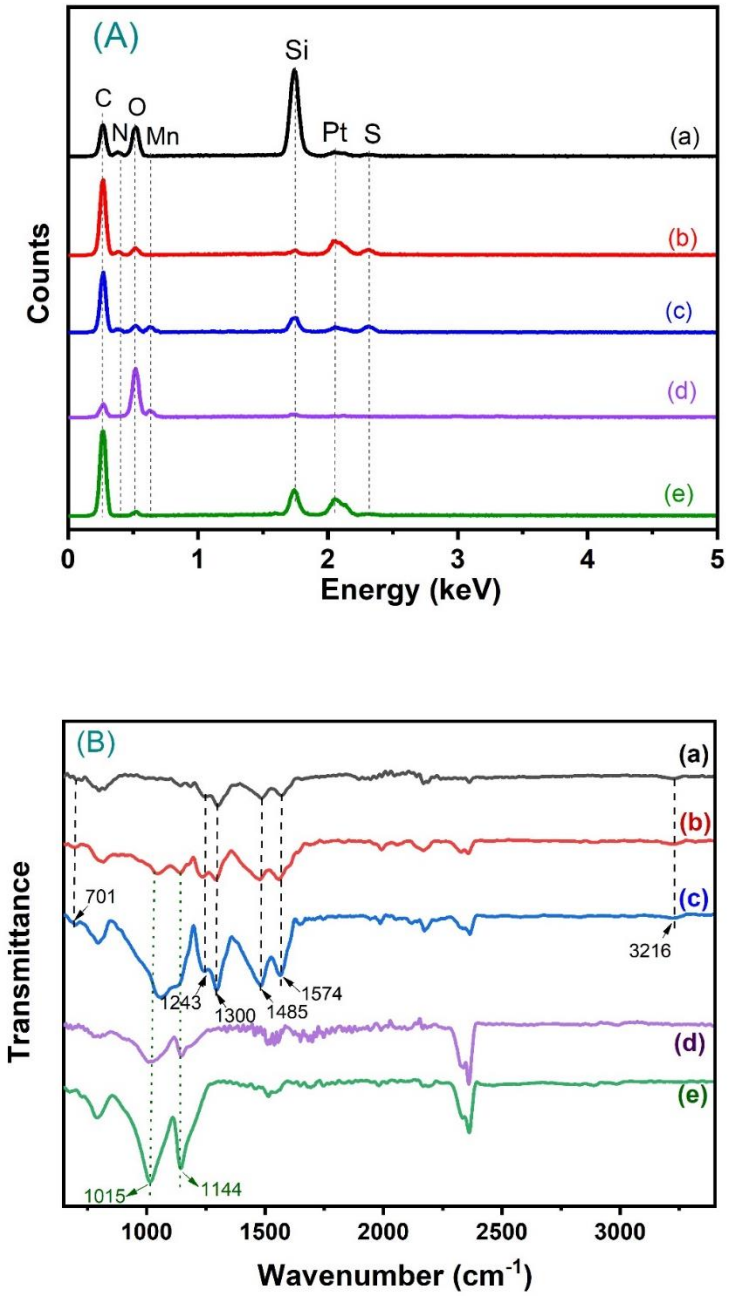

Figure 4. (A) EDX spectra and (B) FT-IR spectra of (a) PANi NWs; (b) MWCNTs/PANi NWs; (c) MWCNTs/MnO_2/PANi NWs; (d) MWCNTs/MnO_2; and (e) MWCNTs on the surface of the Pt electrodes.

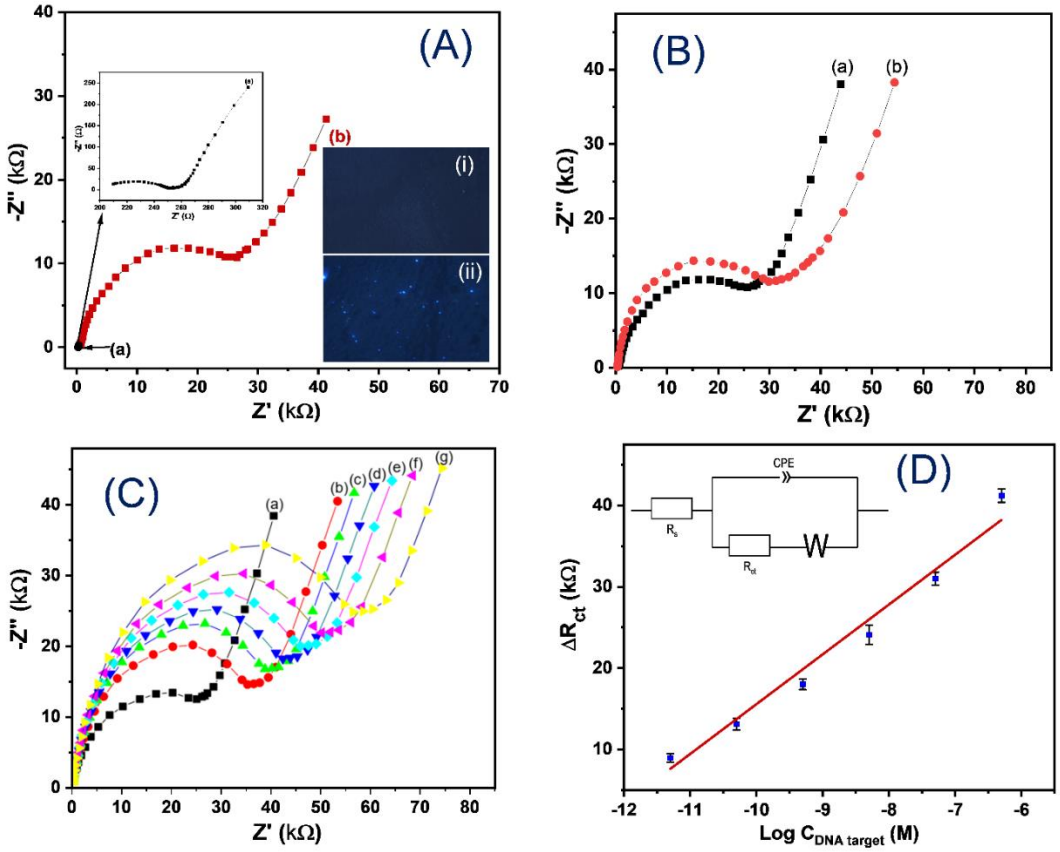

Figure 5. (A) EIS spectra of the Pt/MWCNTs/MnO_2/PANi NWs electrode (a) before and (b) after DNA capture probe immobilization (inserted figure: (a) EIS spectrum of the Pt/MWCNTs/MnO_2/PANi NWs electrode; (i, ii) Fluorescence images of (i) Pt/MWCNTs/MnO_2/PANi NWs; and (ii) Pt/MWCNTs/MnO_2/PANi NWs/DNA probe electrode, respectively); (B) EIS spectra of the DNA sensors (a) before, and (b) after DNA hybridization with the non-complementary target DNA (50 nM); (C) EIS spectra of the DNA sensors after hybridization with different concentrations of the complementary target DNA: (a) 0 pM, (b) 5 pM, (c) 50 pM, (d) 500 pM, (e) 5 nM, (f) 50 nM, and (g) 500 nM; (D) Changes on R_{ct} (ΔR_{ct}) of the DNA sensors vs. concentrations of DNA target (inset: Randles equivalent circuit which is fitted with obtained EIS spectra). Experimental conditions: EIS spectra were measured in PBS buffer (pH 7.4) solution consisted 0.1 M KCl and DNA target sequences. Frequency range: 10^4 Hz to 0.1 Hz, E_{AC} = 5 mV and E_{DC} = 230 mV.

Figures

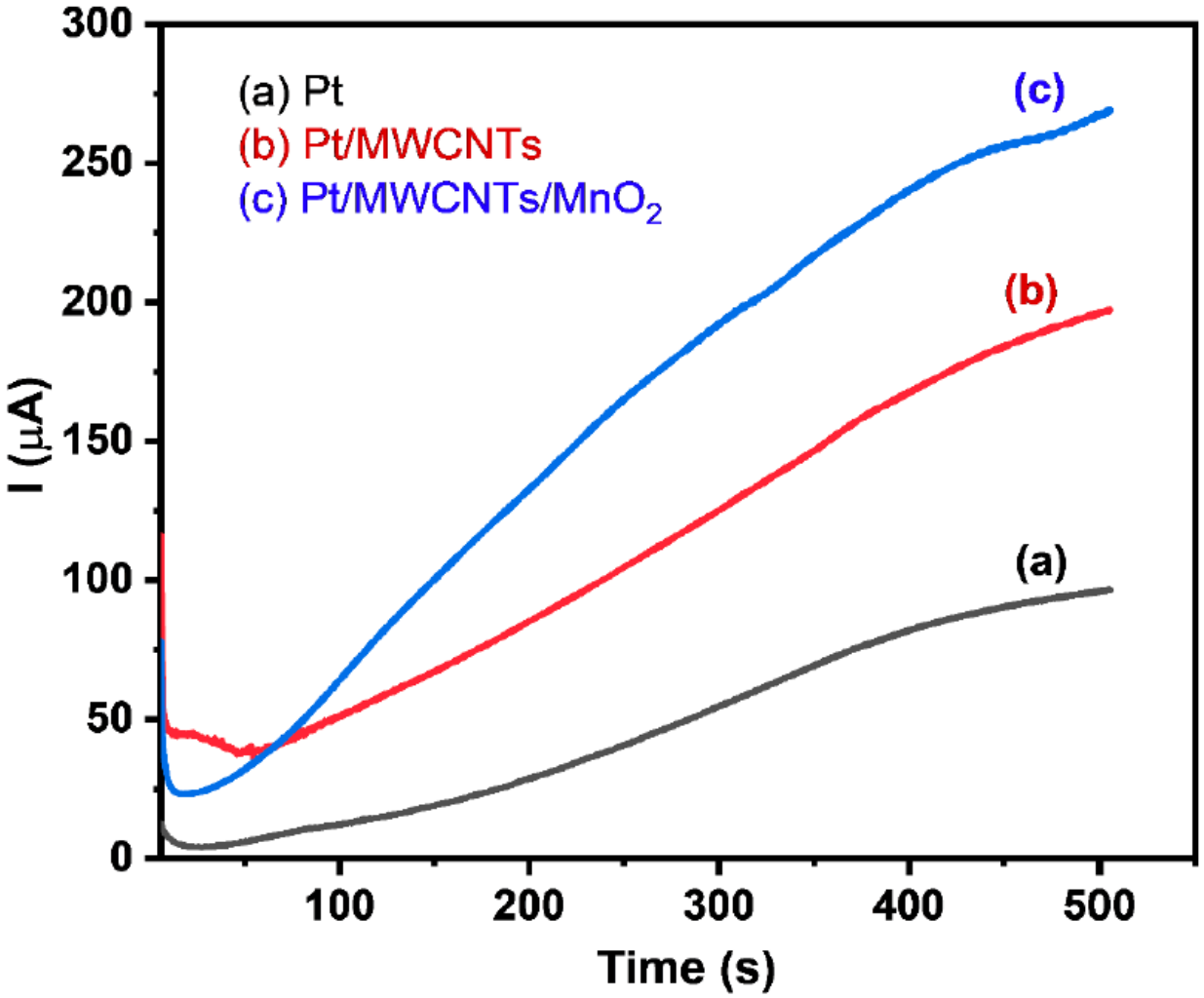

Figure 1

CA results of (a) a bare Pt electrode, (b) a MWCNTs modified Pt electrode (Pt/MWCNTs) and (c) a MWCNTs/MnO2 modified Pt electrode (Pt/ MWCNTs/MnO2). Experimental conditions: the CA curves were recorded in solution containing of 0.05 M aniline monomer and 0.5 M H2SO4 with an applied voltage of 0.9 V vs. SCE at room temperature.

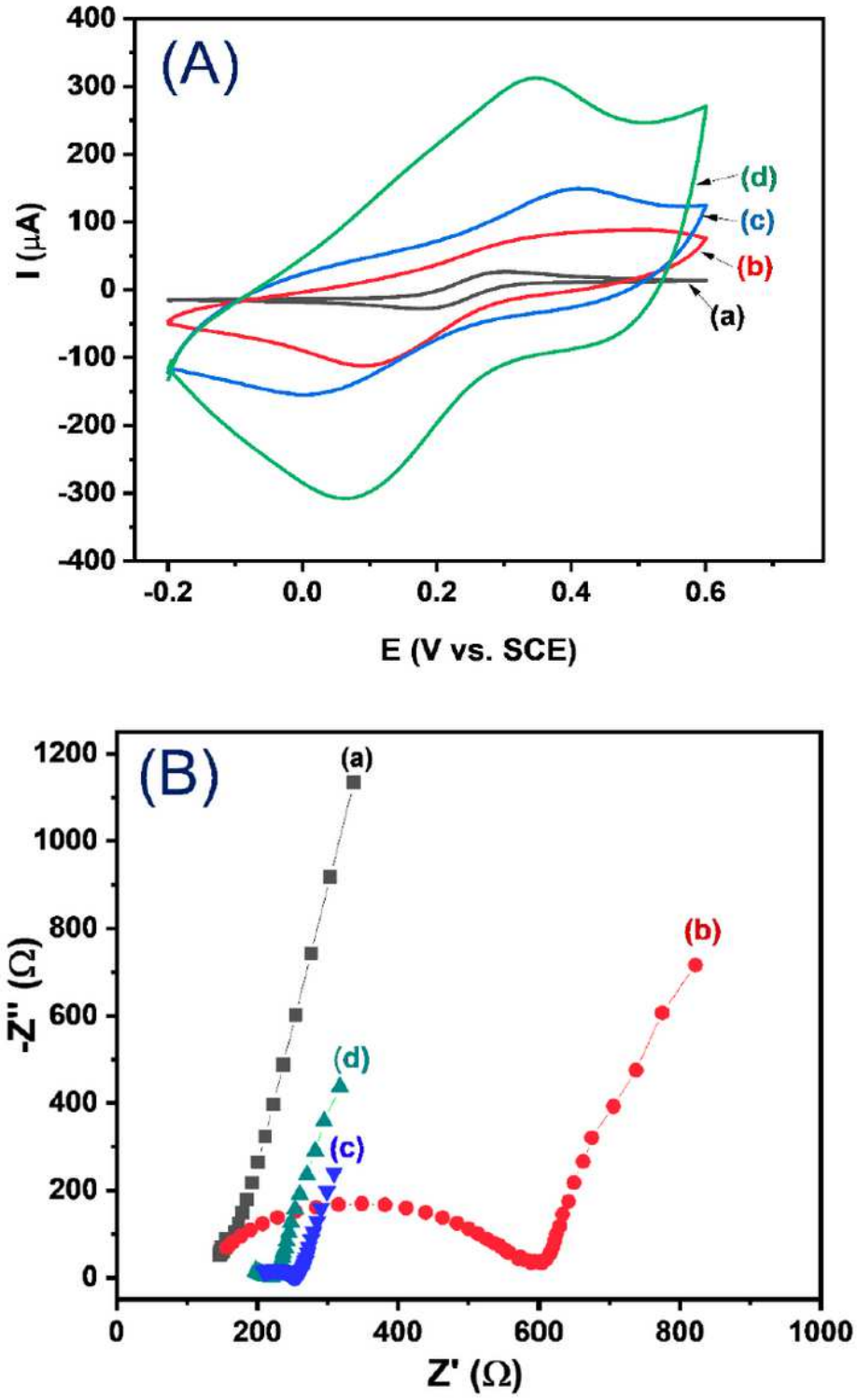

Figure 2

(A) CV results and (B) EIS spectra of (a) bare Pt electrode, and modified Pt electrodes with: (b) MWCNTs, (c) MWCNTs/PANi NWs and (d) MWCNTs/MnO2/PANi NWs films. Experimental conditions: CV and EIS were measured in K3Fe(CN)6/K4Fe(CN)6 (0.005 M) and 0.1 M KCl solution. The CV was recorded at 25 mV s-1 scan rate. The EIS was measured with frequency range: 104 Hz to 0.1 Hz, EAC = 5 mV and EDC = 230 mV.

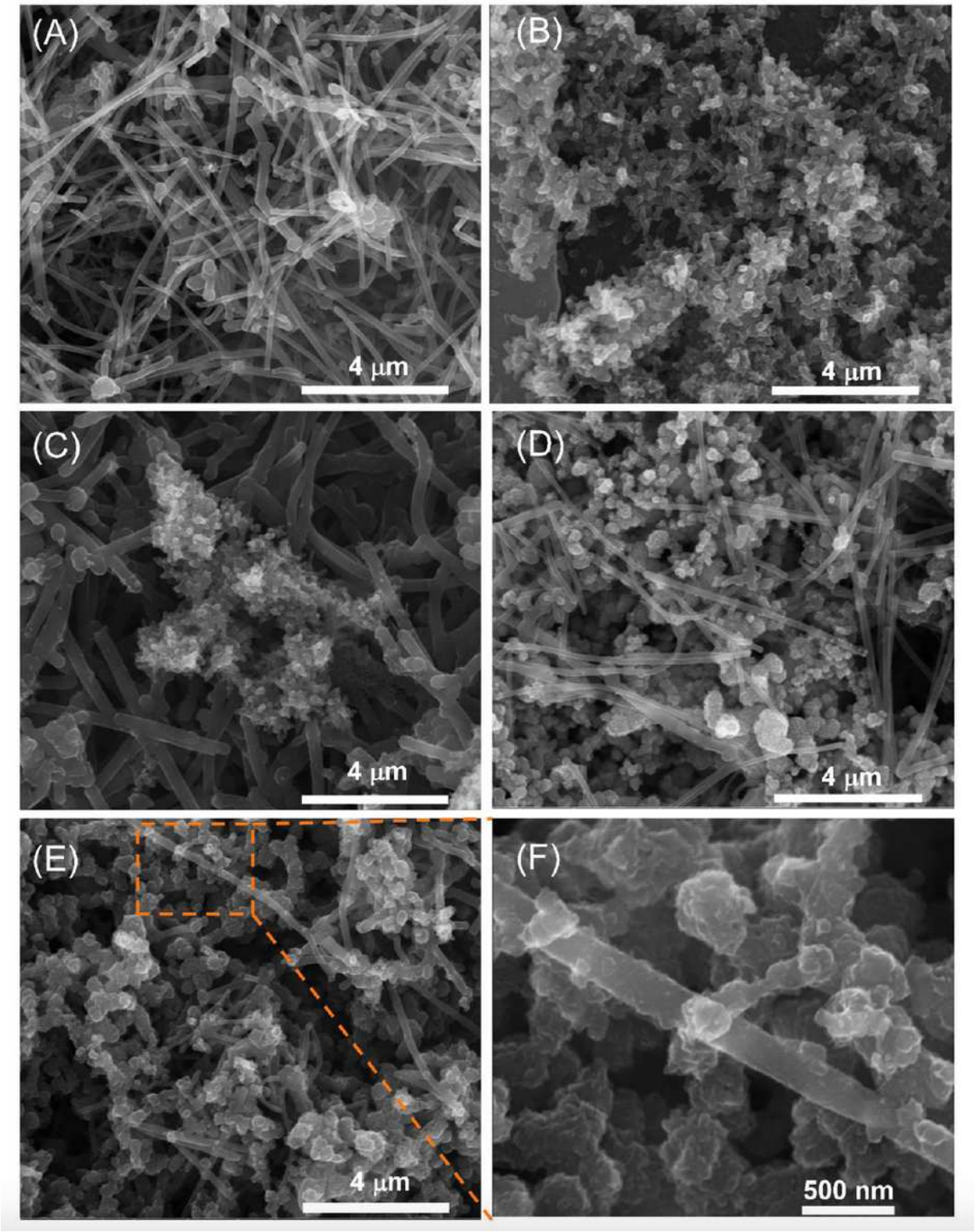

Figure 3

SEM images of (A) MWCNTs; (B) PANi NWs; (C) MWCNTs/PANi NWs; (D) MWCNTs/MnO2; (E, F) MWCNTs/MnO2/PANi NWs on the surface of the Pt electrodes with different magnifications.

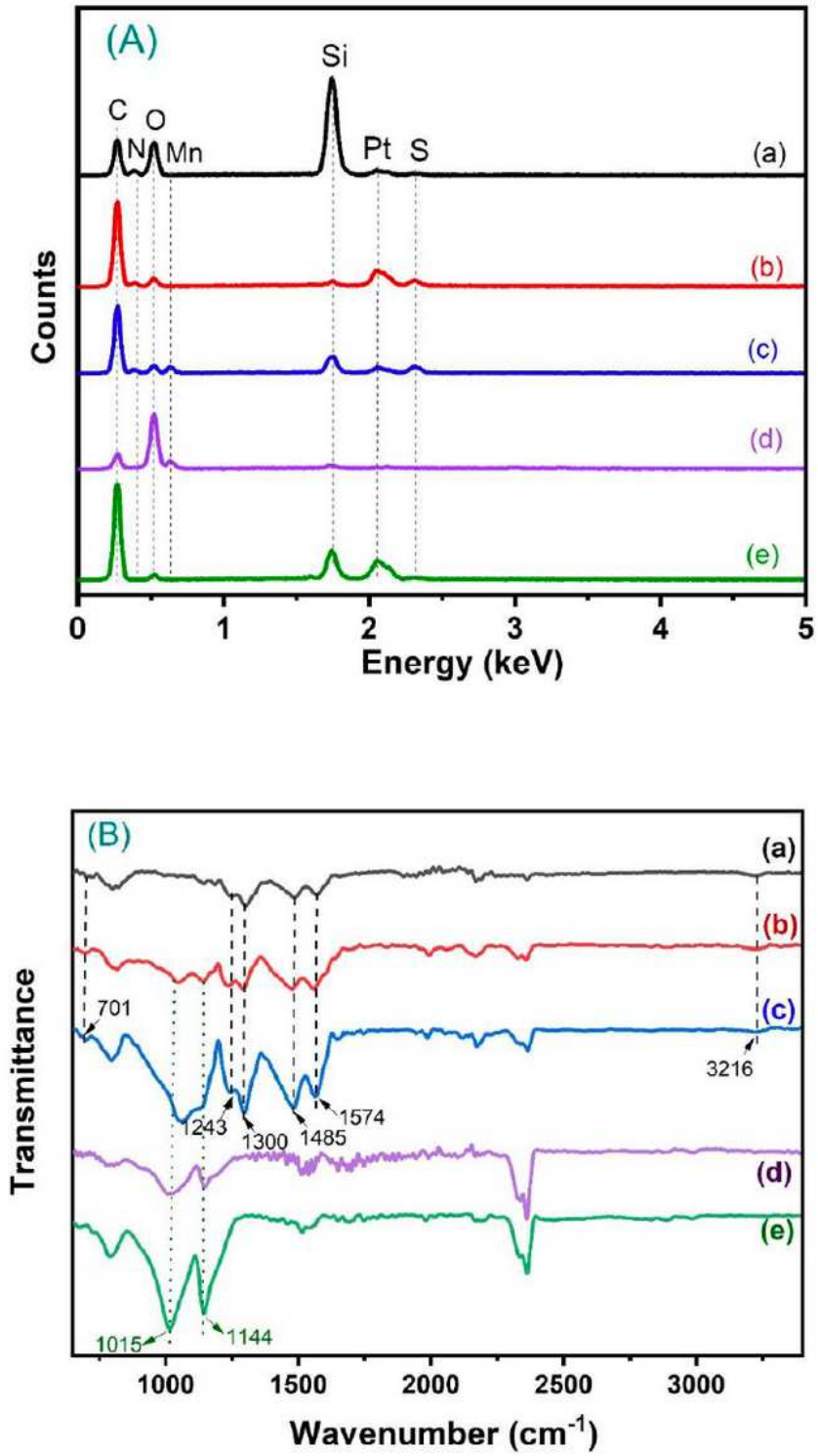

Figure 4

(A) EDX spectra and (B) FT-IR spectra of (a) PANi NWs; (b) MWCNTs/PANi NWs; (c) MWCNTs/MnO2/PANi NWs; (d) MWCNTs/MnO2; and (e) MWCNTs on the surface of the Pt electrodes.

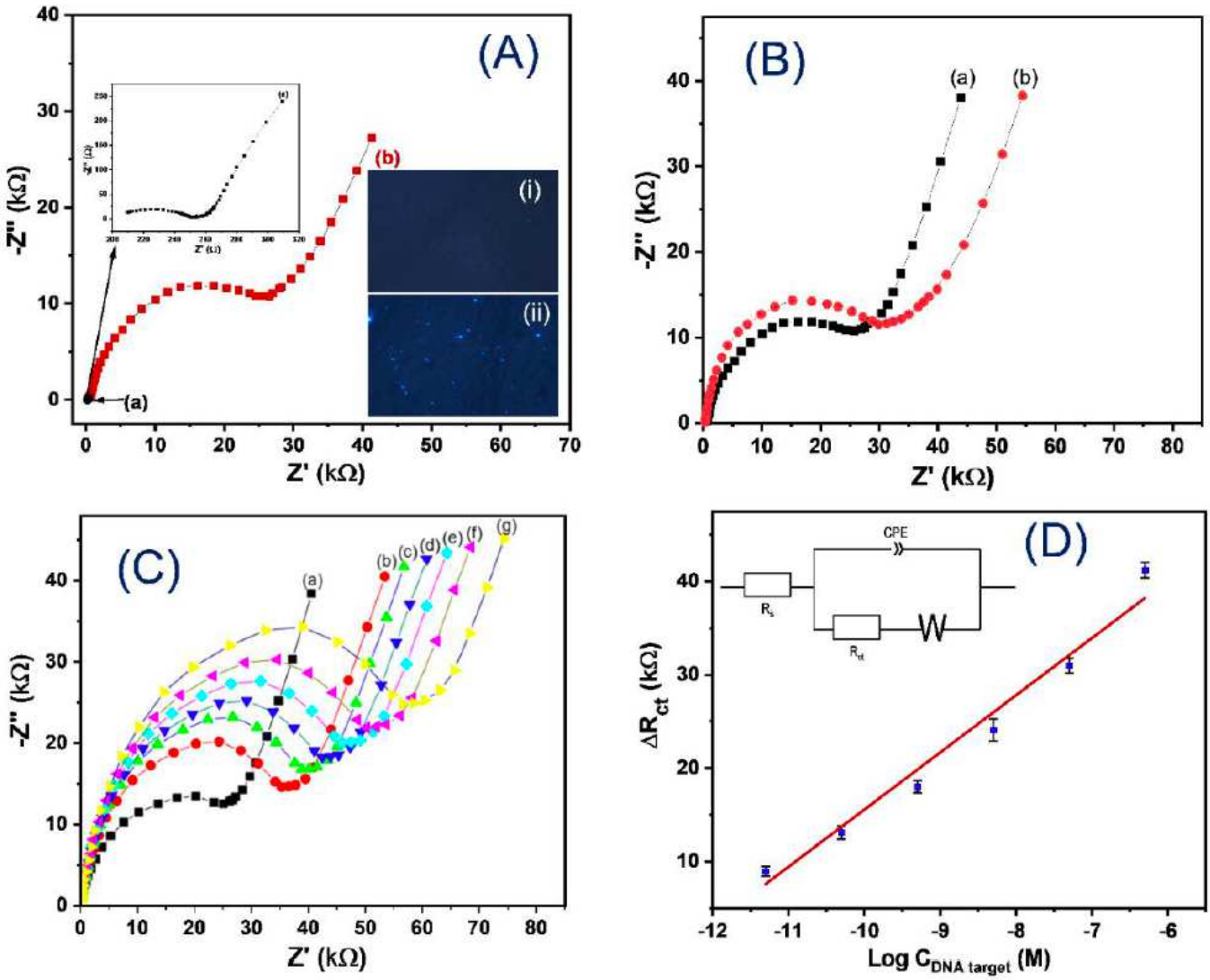

Figure 5

(A) EIS spectra of the Pt/MWCNTs/MnO2/PANi NWs electrode (a) before and (b) after DNA capture probe immobilization (inserted figure: (a) EIS spectrum of the Pt/MWCNTs/MnO2/PANi NWs electrode; (i, ii) Fluorescence images of (i) Pt/MWCNTs/MnO2/PANi NWs; and (ii) Pt/MWCNTs/MnO2/PANi NWs/DNA probe electrode, respectively); (B) EIS spectra of the DNA sensors (a) before, and (b) after DNA hybridization with the non-complementary target DNA (50 nM); (C) EIS spectra of the DNA sensors after hybridization with different concentrations of the complementary target DNA: (a) 0 pM, (b) 5 pM, (c) 50 pM, (d) 500 pM, (e) 5 nM, (f) 50 nM, and (g) 500 nM; (D) Changes on Rct (ΔRct) of the DNA sensors vs. concentrations of DNA target (inset: Randles equivalent circuit which is fitted with obtained EIS spectra). Experimental conditions: EIS spectra were measured in PBS buffer (pH 7.4) solution consisted 0.1 M KCl and DNA target sequences. Frequency range: 104 Hz to 0.1 Hz, EAC = 5 mV and EDC = 230 mV.